Electronic Supplementary Material (ESI) for Energy & Environmental Science

Supporting Information

Structure-Property Relationships of Porous Materials for Carbon Dioxide Separation and Capture

Christopher E. Wilmer,[1] Omar K. Farha,[2] Youn-Sang Bae,[3,a] Joseph T. Hupp,[2] and Randall Q. Snurr[1,b]

[1]Department of Chemical and Biological Engineering
Northwestern University, 2145 Sheridan Road, Evanston, IL 60208, USA

[2]Department of Chemistry
Northwestern University, 2145 Sheridan Road, Evanston, Illinois 60208, USA

[3]Department of Chemical and Biomolecular Engineering
Yonsei University, 262 Seongsanno, Seodaemun-gu, Seoul 120-749, South Korea

[a] To whom correspondence should be addressed: e-mail mowbae@yonsei.ac.kr
[b] To whom correspondence should be addressed: e-mail snurr@northwestern.edu

S1. Simulation Details

Grand canonical Monte Carlo simulations. Except for how partial atomic charges were calculated for the MOF atoms (described in detail below), all other details of our molecular simulations follow previously published methods.[1–3] Atomistic grand canonical Monte Carlo (GCMC) simulations were performed to calculate the adsorption of pure CO_2, CH_4 and N_2 at 298 K at the pressures shown in Table S1.1. These data were used to calculate the five adsorbent evaluation criteria described in Table 1 in the manuscript.

Table S1.1 Pressures used in simulations of CO_2, CH_4 and N_2 adsorption.

Gas Species	Pressures (bar)
CO_2	0.01, 0.05, 0.10, 0.50, 2.50
CH_4	0.05, 0.50, 0.90, 2.5, 4.5
N_2	0.09, 0.90

Each calculation used a 1000 cycle equilibration period followed by a 1000 cycle production run. A cycle consists of n Monte Carlo steps; where n is equal to the number of molecules (which fluctuates during a GCMC simulation). All simulations included random insertion, deletion, rotation (except for CH_4 simulations) and translation moves of molecules with equal probabilities. Atoms in the MOFs were held fixed during the simulations. A 2x2x2 unit cell of every MOF was used for the simulations. Fugacities needed to run the GCMC simulations were calculated using the Peng-Robinson equation of state. Reported adsorption data in all figures is based on the absolute (total) amount of gas in the pores, which is close to the excess adsorbed value at the low pressures considered.

Interaction potential. Interaction energies between non-bonded atoms were computed through the Lennard-Jones (LJ) and Coulomb potentials:

$$\mathcal{V}_{ij} = 4\epsilon_{ij}\left(\left(\frac{\sigma_{ij}}{r_{ij}}\right)^{12} - \left(\frac{\sigma_{ij}}{r_{ij}}\right)^{6}\right) + \frac{q_i q_j}{4\pi\epsilon_0 r_{ij}}$$

where i and j are interacting atoms, and r_{ij} is the distance between atoms i and j, ϵ_{ij} and σ_{ij} are the LJ well depth and diameter, respectively, q_i and q_j are the partial charges of the interacting atoms, and ϵ_0 is the dielectric constant. LJ parameters between different types of sites were calculated using the Lorentz-Berthelot mixing rules. The LJ cutoff distance was 12.8 angstroms, and Ewald sums were used for Coulombic interactions.

MOF model. LJ parameters for the framework atoms were taken from the Universal Force Field (UFF).[4] Table S1.2 shows the LJ parameters for framework atom types used in the hypothetical MOFs.

Table S1.2 LJ parameters for framework atoms in all hypothetical MOFs.

Atom type	σ (Å)	ε/k_B (K)
C	3.43	52.83
O	3.12	30.19
H	2.57	22.14
N	3.26	34.72
F	2.997	25.16
Cl	3.517	114.23
Br	3.73	126.30
Zn	2.46	62.40
Cu	3.114	2.516
V	2.80	8.05
Zr	2.783	34.72

Carbon dioxide model. Partial charges and LJ parameters for CO_2 were taken from the TraPPE force field.[5] This force field has been fit to reproduce the vapor-liquid coexistence curves by Siepmann and co-workers. The CO_2 molecule is modeled as a rigid and linear structure. Table S1.3 shows the LJ parameters and partial charges for CO_2.

Table S1.3. LJ parameters and partial charges for the sites in the carbon dioxide molecule.

Atom type	σ (Å)	ε/k_B (K)	q (e)
C	2.80	27.0	0.70
O	3.05	79.0	-0.35

Methane model. The methane molecules were modeled using the TraPPE force field,[6] which was originally fit to reproduce the vapor-liquid coexistence curve of methane. In this force field, methane is modeled as a single sphere with the parameters shown in Table S1.4.

Table S1.4. LJ parameters for methane molecules.

Atom type	σ (Å)	ε/k_B (K)	q (e)
CH_4 (united)	3.75	148.0	---

Nitrogen model. Nitrogen molecules were modeled using the TraPPE force field,[5] which was originally fit to reproduce the vapor-liquid coexistence curve of nitrogen. In this force field, the nitrogen molecule is a rigid structure where the N-N bond length is fixed at its experimental value of 1.10 Å. This model reproduces the experimental gas-phase quadrupole moment of nitrogen by placing partial charges on N atoms and on a point located at the center of mass (COM) of the molecule. Table S1.5 shows the LJ parameters and partial charges for nitrogen.

Table S1.5. LJ parameters and partial charges for the sites in the nitrogen molecule.

Atom type	σ (Å)	ε/k_B (K)	q (e)
N	3.31	36.0	-0.482
N_2 COM	0	0	0.964

Partial atomic charges. We applied a recently described "extended" charge equilibration (EQeq) algorithm, developed by Wilmer et al.,[3] to obtain partial atomic charges for every framework atom in the database of 137,953 hypothetical MOFs. This new method was required because prior schemes of obtaining partial charges were not sufficiently fast for such a large database. Briefly our method is based on the charge equilibration (Qeq) algorithm developed by Rappé and Goddard[7] where partial charges are assigned such that every atom's desire to hold charge (specified its electronegativity) is balanced by Coulombic attraction/repulsion in the system. In the original Qeq method, hydrogen atoms resisted charge separation via an energy term of cubic order (with respect to charge), which had the consequence that no matter how close in space a pair of oppositely charged atoms were, the Coulombic attraction term of quadratic order would never become infinitely large. While this prevents the unphysical possibility of infinite charge separation, a negative consequence of using higher than quadratic energy terms is that the Qeq method requires iterative computation to converge on the final answer. In contrast, the EQeq method uses only quadratic terms and solves the charge assignment problem non-iteratively. This approach is orders of magnitude faster but runs the risk that, for certain cases, infinite charge separation can occur. To mitigate this possibility, the EQeq method uses a global dielectric constant, ϵ, that weakens charge separation energy terms. In our first report of this method, we examined 14 MOFs and found that $\epsilon = 1.67$ led to partial charges in good agreement with quantum chemistry based methods (specifically the REPEAT method[8]). In this work, we found that the dielectric constant needed to be higher in order to prevent infinite charge separation from occurring on some MOFs. A value of $\epsilon = 2$ led to only 301, out of the 137,953 structures suffering from infinite charge separation, although the predicted partial charges for the remaining structures are expected to be lower in magnitude than what might have been predicted by quantum chemistry based techniques. As a consequence, CO_2 adsorption may be under predicted to some degree in all MOFs. N_2 adsorption may also be affected, although it tends to be less sensitive to the framework charges due to its smaller quadrupole moment.

S2. Description of Plotting Method Used in Manuscript

Our analysis is based on data obtained from gas adsorption simulations, and a variety of supporting calculations (e.g., to obtain the geometric surface area), on over 137,000 hypothetical MOFs. It is a challenge to visualize the results of such a large dataset. One simple method is to depict each MOF as a point, as shown in Figure S2.1a, which was our approach in prior reports.[2,9] However, due to the number of MOFs, the points can overlap significantly and it is difficult to distinguish between regions where there are tens as opposed to thousands of points. In this work, we have used 2D histograms, where the plot domain is divided into *N*x*N* regions (where *N* has been specified in the caption of each figure in the manuscript) and each region is represented by a colored circle, as shown in Figure S2.1b and Figure S2.1c. The colored circle is then used to depict information about the MOFs found within that region, such as the number of MOFs (Figure S2.1b) or the average void fraction (Figure S2.1c). The opacity of each colored circle can vary independently of the hue, and so can provide additional information. In Figure S2.1b every circle is 100% opaque, but in Figure S2.1c the opacity is a function of the MOF count in the corresponding region. If the number of MOFs is less than *X*, the circle has an opacity of 0% (i.e., no circle is drawn), whereas if the number of MOFs is greater that *Y*, the opacity of the circle is 100% (opacity varies linearly between *X* and *Y*).

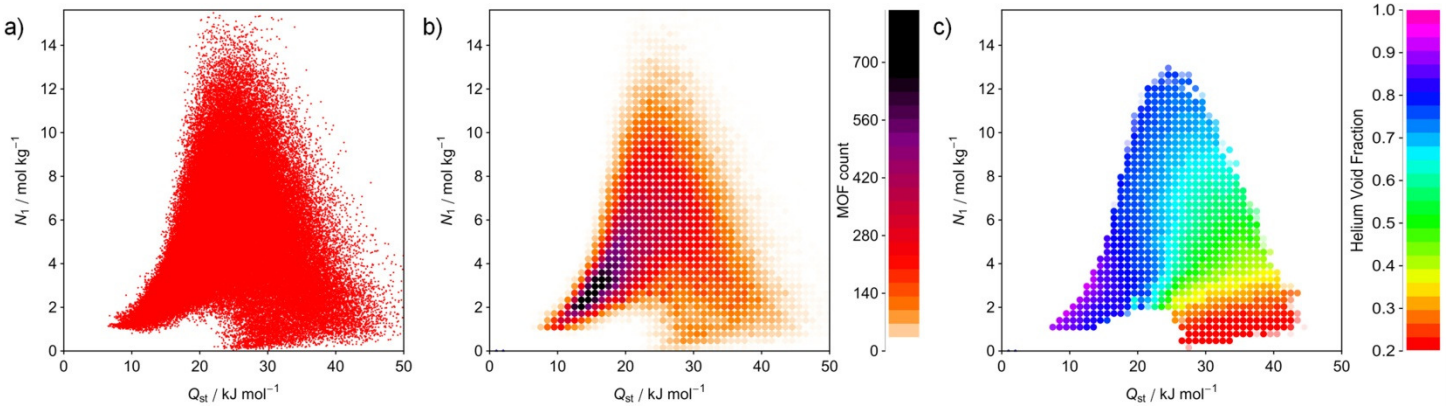

Fig. S2.1 Three, of many, approaches to visualize data of simulated properties in over 137,000 MOFs. Here, the CO_2 uptake at the adsorption pressure (N_1) for Case 2 (landfill gas separation) is plotted against the CO_2 heat of adsorption (Q_{st}) in three different ways, a) as a scatter plot where each MOF is shown as a point, b) as a 2D histogram where the color of each circle indicates the number of MOFs in that region, and c) as a 2D histogram where the color of each circle represents the average void fraction of the MOFs in that region. In both 2D histograms, the plot region has been divided in 50x50 regions. Additionally, in c) the opacity of each colored circle is determined by the number of MOFs in that region. If less than 25 MOFs are found in the region represented by the circle the opacity is 0% (i.e., no circle is drawn) and increases by 10% for each additional MOF so that the circle is fully opaque if there are greater than 35 MOFs.

In the accompanying manuscript, all figures showing structure-property relationships use the approach in Figure S2.1c. For each figure, the number of regions *N*x*N* is indicated, as well as the threshold value *X* at which the opacity of the circles begins to increase. For all figures, the opacity increases by 10% for each MOF above the *X* value provided in the caption.

The primary benefit of this visualization approach is to identify trends in structure-property relationships that might otherwise be obscured by noise. A point of caution should be made on the interpretation of the color in these figures, namely that the color represents the *mean value* of some property for all MOFs in that region. If the MOFs in that region fall into two distinct groups (e.g., 500 MOFs with void fractions of ~0.4 and 500 MOFs with void fractions ~0.8), the color of the circle may correspond to an average value that is not representative of any of the MOFs in that region (i.e., a void fraction of ~0.6). Similarly, any complex distribution of property values within the plot region represented by one circle will not be accurately portrayed by its color.

S3. Additional Structure-Property Relationships

In the accompanying manuscript we plotted a few of the many possible structure-property combinations resulting from our large-scale screening. In particular, only four of the five adsorbent evaluation criteria were plotted against Q_{st} and gravimetric surface area. Here we plot, for the sake of completeness, the CO_2 uptake at the adsorption pressure, N_1, against Q_{st} and gravimetric surface area (see Fig. S3.1). Additionally, we show on the following pages how the five adsorbent evaluation criteria vary with volumetric surface area (Fig. S3.2), maximum pore diameter (Fig. S3.3) and density (Fig. S3.4).

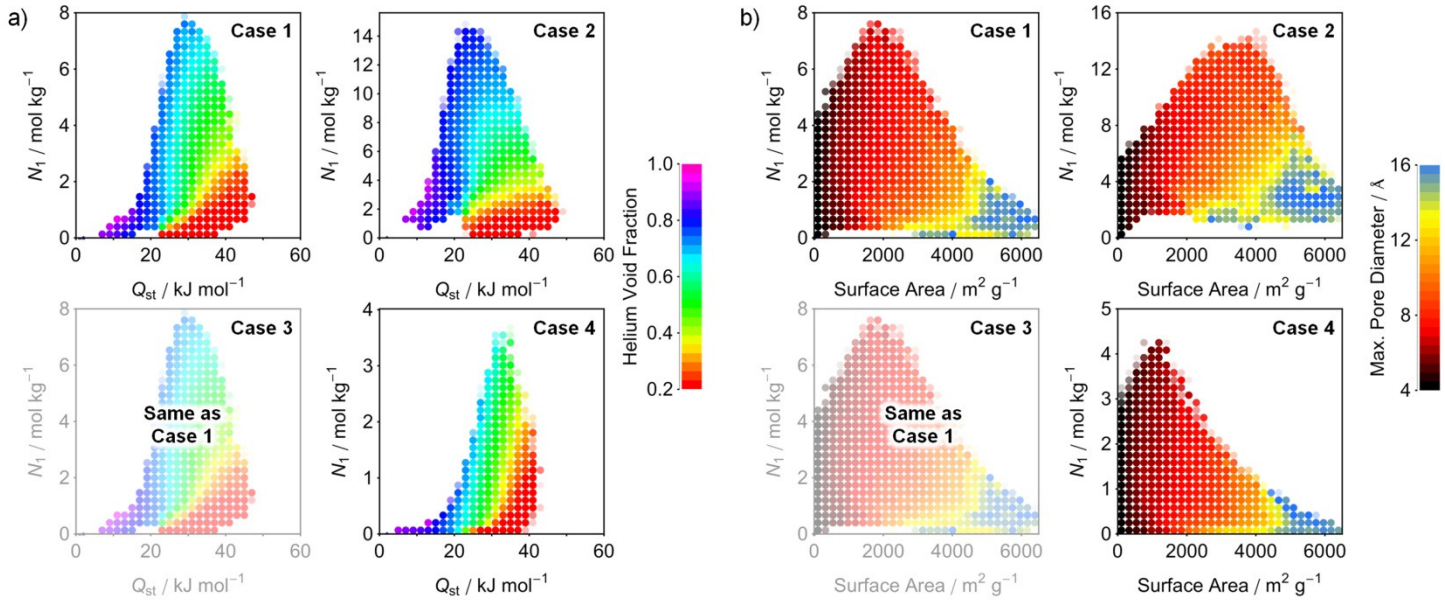

Fig. S3.1 The relationship between CO_2 uptake at the adsorption pressure (N_1) and a) the heat of adsorption (Q_{st}) of CO_2, as well as b) gravimetric surface area for each of the four cases. Each plot is divided into 30x30 regions that are represented by a filled circle if more than 10 structures exist within that region. Although the adsorption pressure is different for Case 1 and Case 3 (5 bar and 1 bar, respectively), the partial pressure of CO_2 in the mixture gas is the same and so N_1 is identical for both cases.

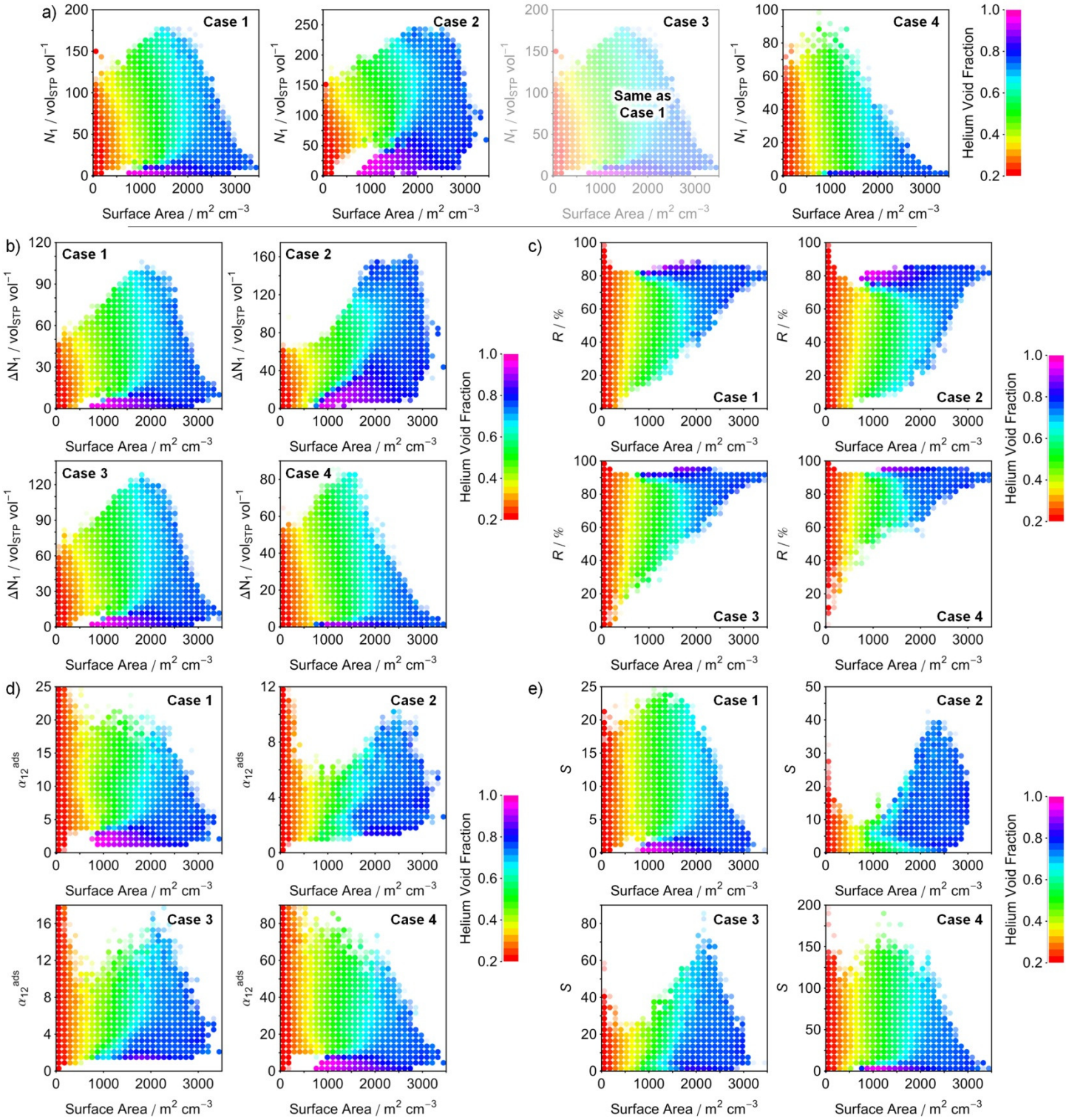

Fig. S3.2 The relationships between a) the CO_2 uptake at the adsorption pressure (N_1), b) working capacity (ΔN_1), c) regenerability (R), d) selectivity (α_{12}^{ads}) and e) sorbent selection parameter (S) and the volumetric surface area for each of the four cases. Each plot is divided into 30x30 regions that are represented by a filled circle if more than 10 (or 25 for S values due to higher statistical error that results from being an aggregate of the other parameters) structures exist within the region. Although the adsorption pressure is different for Case 1 and Case 3 (5 bar and 1 bar, respectively), the partial pressure of CO_2 in the mixture gas is the same and so N_1 is identical for both cases.

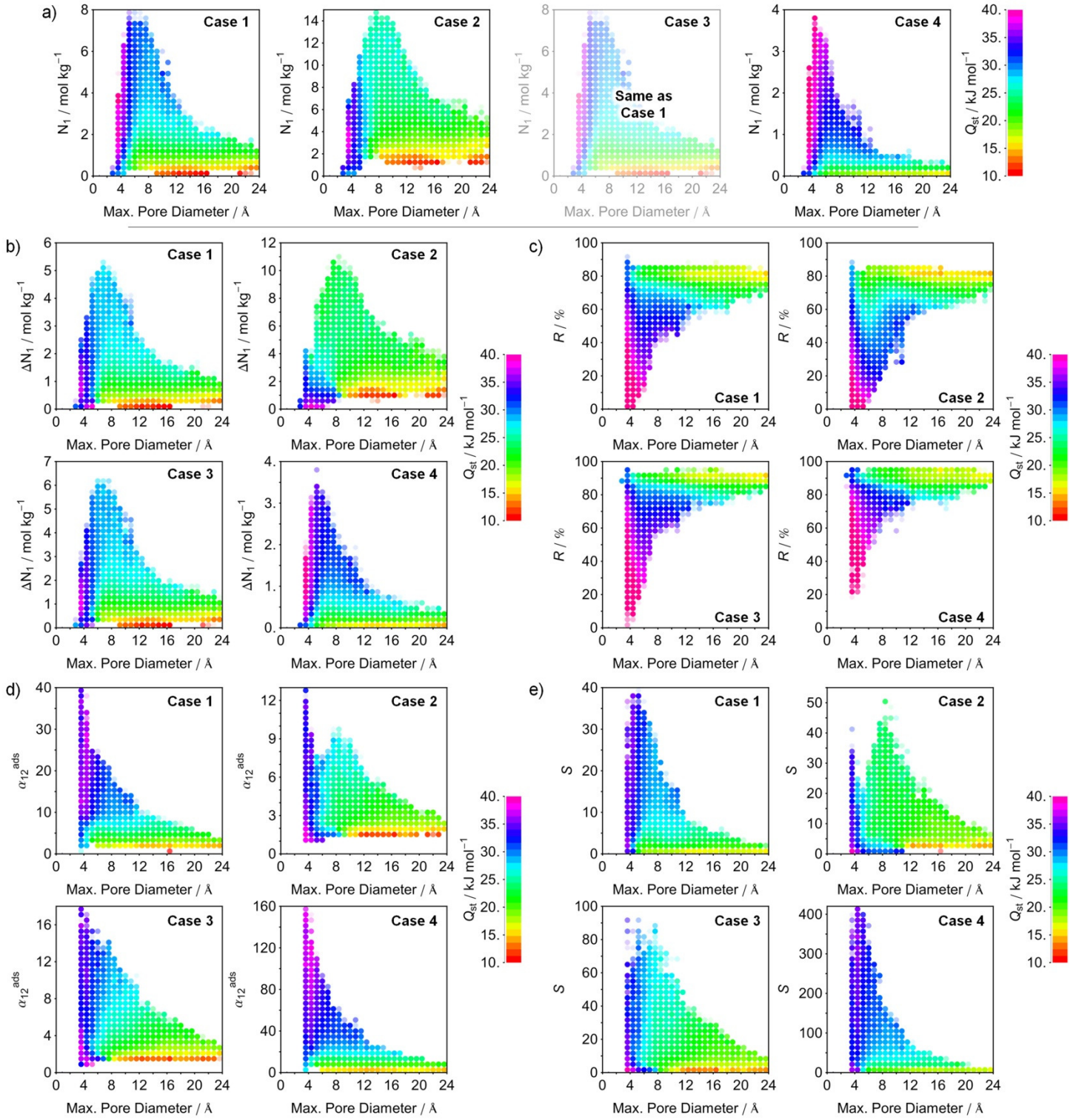

Fig. S3.3 The relationships between a) the CO_2 uptake at the adsorption pressure (N_1), b) working capacity (ΔN_1), c) regenerability (R), d) selectivity (α_{12}^{ads}) and e) sorbent selection parameter (S) and the maximum pore diameter for each of the four cases. Each plot is divided into 30x30 regions that are represented by a filled circle if more than 10 (or 25 for α_{12}^{ads} and S values due to higher statistical error that results from being an aggregate of the other parameters) structures exist within the region. Although the adsorption pressure is different for Case 1 and Case 3 (5 bar and 1 bar, respectively), the partial pressure of CO_2 in the mixture gas is the same and so N_1 is identical for both cases.

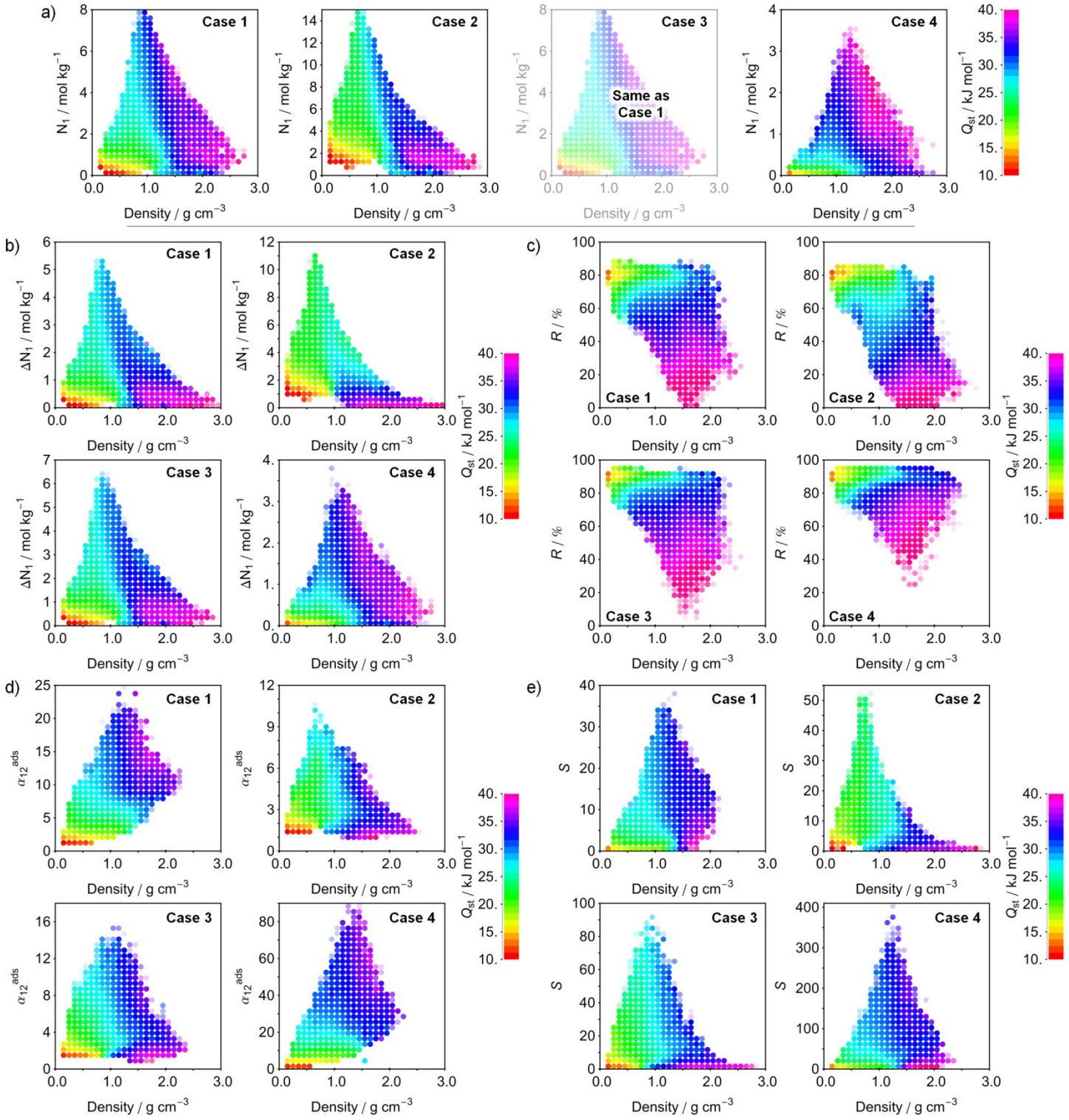

Fig. S3.4 The relationships between a) the CO_2 uptake at the adsorption pressure (N_1), b) working capacity (ΔN_1), c) regenerability (R), d) selectivity (α_{12}^{ads}) and e) sorbent selection parameter (S) and the material density for each of the four cases. Each plot is divided into 30x30 regions that are represented by a filled circle if more than 10 (or 25 for α_{12}^{ads} and S values due to higher statistical error that results from being an aggregate of the other parameters) structures exist within the region. Although the adsorption pressure is different for Case 1 and Case 3 (5 bar and 1 bar, respectively), the partial pressure of CO_2 in the mixture gas is the same and so N_1 is identical for both cases.

References:

1. A. Ö. Yazaydin, R. Q. Snurr, T. H. Park, K. Koh, J. Liu, M. D. LeVan, A. I. Benin, P. Jakubczak, M. Lanuza, D. B. Galloway, J. J. Low, and R. R. Willis, *J. Am. Chem. Soc.*, 2009, **131**, 18198–18199.
2. C. E. Wilmer, M. Leaf, C.-. Y. Lee, O. K. Farha, B. G. Hauser, J. T. Hupp, and R. Q. Snurr, *Nat. Chem.*, 2012, **4**, 83–89.
3. C. E. Wilmer, K.-C. Kim, and R. Q. Snurr, *submitted.*, 2012.
4. A. K. Rappé, C. J. Casewit, K. S. Colwell, W. A. Goddard III, and W. M. Skiff, *J. Am. Chem. Soc.*, 1992, **114**, 10024–10035.
5. J. J. Potoff and J. I. Siepmann, *AIChE J.*, 2001, **47**, 1676–1682.
6. M. G. Martin and J. I. Siepmann, *J. Phys. Chem. B*, 1998, **102**, 2569–2577.
7. A. K. Rappé and W. A. Goddard III, *J. Phys. Chem.*, 1991, **95**, 3358–3363.
8. C. Campañá, B. Mussard, and T. K. Woo, *J. Comp. Chem.*, 2009, **5**, 2866–2878.
9. B. J. Sikora, C. E. Wilmer, M. L. Greenfield, and R. Q. Snurr, *Chem. Sci.*, 2012, **3**, 2217–2223.